PHYSICAL REVIEW B **89**, 121101(R) (2014)

Orbital occupancies and the putative $j_{\rm eff} = \frac{1}{2}$ ground state in Ba_2IrO_4: A combined oxygen K-edge XAS and RIXS study

M. Moretti Sala,[1,*] M. Rossi,[1] S. Boseggia,[2,3] J. Akimitsu,[4] N. B. Brookes,[1] M. Isobe,[5] M. Minola,[6] H. Okabe,[5] H. M. Rønnow,[7] L. Simonelli,[1] D. F. McMorrow,[2] and G. Monaco[8,1]

[1]*European Synchrotron Radiation Facility, BP 220, F-38043 Grenoble Cedex, France*

[2]*London Centre for Nanotechnology and Department of Physics and Astronomy, University College London, London WC1E 6BT, United Kingdom*

[3]*Diamond Light Source Ltd, Diamond House, Harwell Science and Innovation Campus, Didcot, Oxfordshire OX11 0DE, United Kingdom*

[4]*Department of Physics and Mathematics, Aoyama Gakuin University, 5-10-1 Fuchinobe, Chuo-ku, Sagamihara, Kanagawa 252-5258, Japan*

[5]*National Institute for Materials Science (NIMS), 1-1 Namiki, Tsukuba, Ibaraki 305-0044, Japan*

[6]*CNR-SPIN, CNISM and Dipartimento di Fisica, Politecnico di Milano, Piazza Leonardo da Vinci 32, I-20133 Milano, Italy*

[7]*Laboratory for Quantum Magnetism, École Polytechnique Fédérale de Lausanne (EPFL), CH-1015, Switzerland*

[8]*Dipartimento di Fisica, Università di Trento, via Sommarive 14, 38123 Povo (TN), Italy*

(Received 3 December 2013; published 3 March 2014)

The nature of the electronic ground state of Ba_2IrO_4 has been addressed using soft x-ray absorption and inelastic scattering techniques in the vicinity of the oxygen K edge. From the polarization and angular dependence of x-ray absorption spectroscopy (XAS) we deduce an approximately equal superposition of xy, yz, and zx Ir^{4+} $5d$ orbitals. By combining the measured orbital occupancies, with the value of the spin-orbit coupling provided by resonant inelastic x-ray scattering (RIXS), we estimate the crystal field splitting associated with the tetragonal distortion of the IrO_6 octahedra to be small, $\Delta \approx 50(50)$ meV. We thus conclude definitively that Ba_2IrO_4 is a close realization of a spin-orbit Mott insulator with a $j_{\rm eff} = \frac{1}{2}$ ground state, thereby overcoming ambiguities in this assignment associated with the interpretation of x-ray resonant scattering experiments.

DOI: 10.1103/PhysRevB.89.121101 PACS number(s): 71.27.+a, 71.70.Ej, 78.70.Dm

The comprehensive characterization of the ground state of a system forms the basis for understanding its physical properties. In the case of the new class of spin-orbit induced Mott insulating iridium oxides, the so-called $j_{\rm eff} = \frac{1}{2}$ ground state has been proposed to explain the unexpected transport properties of Sr_2IrO_4 (and related compounds) [1,2] and is more generally central to the prediction of the novel electronic phases in iridates. Naively one might predict that a $5d$ transition-metal oxide (TMO) would be metallic because of the large extension of its orbitals and reduced electronic correlations. However, the large spin-orbit coupling present in the $5d$ transition metal leads to the lifting of degeneracies in the ground state manifold, allowing diminished electronic correlations to play an enhanced role. Accordingly, Sr_2IrO_4 turns out in fact to be an antiferromagnetic insulator with properties reminiscent of $3d$ TMO Mott insulators [3]. The realization of the $j_{\rm eff} = \frac{1}{2}$ ground state is subject to tight constraints on the energies at play. Ba_2IrO_4 displays similar transport properties with respect to the most studied Sr_2IrO_4, but also significant structural differences [4] which may alter the relevant energy scales. Whether or not the insulating behavior of Ba_2IrO_4 can be explained within the framework of the $j_{\rm eff} = \frac{1}{2}$ model is therefore unclear.

Valuable insight into the physics of Sr_2IrO_4 and related materials can be obtained within the frame of a single-ion model, in which $5d$ e_g states are neglected and one *hole* fills the t_{2g} states, which are subject to tetragonal crystal field splitting (Δ) and spin-orbit coupling (ζ) [5–8]. For magnetic moments oriented along the (110) direction, the ground state wave function is written as [9]

$$|0,-\rangle = \frac{C_0(|xy,+\rangle - \imath|xy,-\rangle)/\sqrt{2} + |yz,-\rangle + \imath|zx,+\rangle}{\sqrt{2+C_0^2}}, \tag{1}$$

with $2C_0 = \delta - 1 + \sqrt{9+\delta(\delta-2)}$ ($C_0 \geqslant 0$), where $\delta = 2\Delta/\zeta$. Theoretically, a pure $j_{\rm eff} = \frac{1}{2}$ ground state is realized for $\Delta = 0$ only, with an equal occupation of the xy, yz, and zx orbitals. Instead, for $\Delta \gg \zeta$ the $(|xy,+\rangle - \imath|xy,-\rangle)/\sqrt{2}$ state is stabilized, while for $\Delta \ll -\zeta$ the ground state reduces to $(|yz,+\rangle + \imath|zx,-\rangle)/\sqrt{2}$.

Compelling, microscopic evidence for the existence of a $j_{\rm eff} = \frac{1}{2}$ ground state in iridium oxides was first provided by x-ray resonant magnetic scattering (XRMS) experiments. It was argued that the near vanishing of the L_2/L_3 magnetic Bragg peak intensity ratio provides a unique signature of the $j_{\rm eff} = \frac{1}{2}$ ground state [10,11]. The subsequent application of XRMS to several compounds led to the identification of a number of other "$j_{\rm eff} = \frac{1}{2}$ iridates," such as $Sr_3Ir_2O_7$ [11–13], Ba_2IrO_4 [14], $CaIrO_3$ [7], and Ca_4IrO_6 [15]. However, early on Chapon and Lovesey [16] raised doubts on this interpretation. More recently, some of the present authors further clarified the situation by showing that the Ir L_2-edge XRMS cross section is identically zero *irrespective* of the tetragonal crystal field splitting of t_{2g} states when the magnetic moments lie in the *ab* plane [9]. Therefore, a zero L_2/L_3 XRMS intensity ratio is a necessary but not sufficient condition for the $j_{\rm eff} = \frac{1}{2}$ ground state to be realized in iridate perovskites with in-plane easy magnetic axis. Sr_2IrO_4 [10] and Ba_2IrO_4 [14] fall exactly in this category.

By now, the $j_{\rm eff} = \frac{1}{2}$ ground state of Sr_2IrO_4 has been verified by a number of experimental techniques, including

*marco.moretti@esrf.fr

optical conductivity, O K-edge XAS, ARPES [2], XRMS [10], and RIXS [17,18], and the tetragonal crystal field has been shown to be small [19]. Like the benchmark compound, it was suggested that Ba_2IrO_4 is a spin-orbit Mott insulator [4], and indeed recent ARPES measurements suggest that Sr_2IrO_4 and Ba_2IrO_4 have qualitatively similar band structures [20]. The crystal structure and the magnetic properties of the two compounds, however, are significantly different. In both Sr_2IrO_4 and Ba_2IrO_4 the apical Ir-O bonds are longer than the in-plane bonds, but with differences of 4% and 7%, respectively [3,4], implying a larger tetragonal distortion in the latter compound. Additionally, in Sr_2IrO_4 the IrO_6 octahedra have a staggered rotation about the c axis by $\sim 12^\circ$ [3], such that the in-plane Ir-O-Ir angles are not 180°, while in Ba_2IrO_4 the Ir-O-Ir bonds are straight [4]. The combination of a larger tetragonal distortion and the absence of octahedra rotation has mainly two effects: (i) the crystal field potential acting on the central Ir ion is different in the two compounds. *Ab initio* quantum chemistry calculations by Hozoi *et al.* [21] show that the local Ir-O bonding sets a different energy order of the Ir t_{2g} levels for the two compounds in the absence of spin-orbit coupling; in the *electron* representation, the lowest, doubly occupied t_{2g} level is xy in Ba_2IrO_4, and yz/zx in Sr_2IrO_4. (ii) The inversion symmetry at the O site between adjacent Ir ions is preserved and Dzyaloshinsky-Moriya-type (DM) interaction is suppressed. DM interaction in Sr_2IrO_4 is responsible for the canting of the magnetic moments, which in turn produces a finite ferromagnetic component below 240 K [10]; Ba_2IrO_4, instead, does not exhibit a net magnetic moment at any temperature [4].

Thus taking into account all of the above facts, the question of whether or not the $j_{\text{eff}} = \frac{1}{2}$ ground state is realized in Ba_2IrO_4 is an interesting but open one. Here we address this question by presenting the results of oxygen K-edge XAS and RIXS which allow us to directly determine the occupancy of the xy, yz, and zx orbitals in the ground state of Eq. (1), and to estimate the tetragonal crystal field.

O K-edge x-ray absorption spectroscopy (XAS) and resonant inelastic x-ray scattering (RIXS) data were taken at the ID08 soft x-ray beam line of the European Synchrotron Radiation Facility, Grenoble. XAS spectra were collected in total-fluorescence-yield mode to ensure the highest bulk sensitivity. RIXS spectra were measured with the AXES spectrometer working at a fixed scattering angle of 130°. The energy resolution of the incident photons was better than 100 meV, while the overall energy resolution of the RIXS spectra was 180 meV, as determined by measuring the off-resonant elastic scattering of amorphous graphite. The photon polarization was set to be either horizontal (H) or perpendicular (V) to the scattering plane. The photons impinge onto the sample at an angle θ with respect to the normal of the sample surface. RIXS measurements were performed at $\theta = 25^\circ$ (specular geometry); in this geometry, spectra taken with horizontal and vertical polarization (4 h each) were found to be similar, and therefore were summed up to reduce the error bars. The temperature of the sample was kept below 50 K during the whole experiment. The sample, a single crystal of Ba_2IrO_4 (of $\sim 0.5 \times 0.5 \times 0.2$ mm^3 size), synthesized at the National Institute for Materials Science (NIMS) by the slow cooling technique under pressure [4], was oriented having the

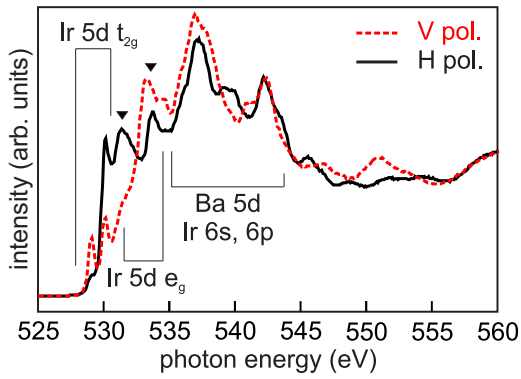

FIG. 1. (Color online) XAS spectra of Ba_2IrO_4 for both horizontal (black continuous line) and vertical (red dashed line) polarization of the photons at $\theta = 80^\circ$.

(010) and (001) crystallographic direction in the horizontal plane. Note that in this geometry the vertical polarization is always parallel to the (100) axis, while the direction of the horizontal polarization relative to the sample changes with θ according to $\boldsymbol{\epsilon}_H = (0, \cos\theta, \sin\theta)$.

Figure 1 shows two representative XAS spectra of Ba_2IrO_4 for both horizontal (black line) and vertical (red line) incident photon polarization at $\theta = 80^\circ$, over an extended energy range from 525 to 560 eV. A linear background was subtracted by fitting the flat region at energies lower than 528 eV; the spectra were then normalized to unity on the high energy side of the edge jump. We clearly observe a pronounced polarization dependence, most notably in the prepeak region, at energies lower than 535 eV. Typically this region is associated with transitions of the O 1s core electrons to the 2p states hybridized with the transition metal ion unoccupied valence states; in our case, these can be mainly associated with the Ir 5d t_{2g} and e_g states. Structures at higher energies are assigned to Ba 5d and Ir 6s and 6p empty states. In Fig. 2 we highlight the polarization and angular dependence of the prepeak region (528 to 533 eV) by focusing on the two peaks at 529.1 and 530.1 eV which arise from O 2p-Ir 5d t_{2g} hybridization. At $\theta = 0$ (left panel) the

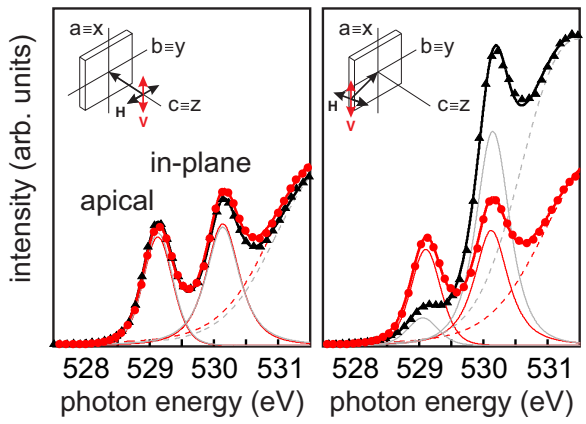

FIG. 2. (Color online) XAS spectra of Ba_2IrO_4 for both horizontal (black triangles) and vertical (red circles) polarization of the photons at (left panel) $\theta = 0^\circ$ and (right panel) $\theta = 80^\circ$. The corresponding experimental geometries are shown in the inset.

spectra taken with the two photon polarizations are essentially identical, while for $\theta = 80^\circ$ (right panel) the spectra are strongly affected by polarization: specifically, the low-energy peak (529.1 eV) is strongly suppressed, while the peak at higher energy (530.1 eV) is strongly enhanced when switching from H to V polarization. This behavior reflects the anisotropy of the orbitals: at $\theta = 0$, $\boldsymbol{\epsilon}_V = (100)$ and $\boldsymbol{\epsilon}_H = (010)$, and the spectra are identical owing to the equivalence of the (100) and (010) directions in Ba_2IrO_4; on the other hand, $\boldsymbol{\epsilon}_V = (100)$, while $\boldsymbol{\epsilon}_H \approx (001)$ at $\theta = 80^\circ$, and the spectra look different as Ba_2IrO_4 has tetragonal symmetry.

Following the work of Moon *et al.* [22] on Sr_2IrO_4, and in agreement with the peak assignments in $La_{2-x}Sr_xCuO_4$ [23], Sr_2RuO_4 [24], and Ca_2RuO_4 [25], the two peaks at 529.1 and 530.1 eV of Fig. 2 arise from transitions to the $5d$ t_{2g} states at the apical and in-plane oxygens, respectively. Also, the broad peaks at 532 and 534 eV (indicated by triangles in Fig. 1) correspond to transitions to the $5d$ $3z^2 - r^2$ and $x^2 - y^2$ states, respectively [22]. With this assignments, 10Dq can be estimated to be about 3 eV in Ba_2IrO_4.

To quantitatively estimate their polarization and angular dependence, the XAS spectra are fitted in Fig. 2 to two Gaussian functions plus a third curve (dashed lines) to account for higher-energy features. While the position and full width half maximum ($\approx$0.55 eV) of the peaks are insensitive to the different geometries, it is interesting to look at the angular and polarization dependence of the corresponding spectral weights: The integrated intensity ratio of the apical and in-plane oxygen contributions is 0.71 (0.69) for vertical (horizontal) polarization at $\theta = 0$, and 0.64 (0.11) at $\theta = 80^\circ$, i.e., the apical oxygen contribution is strongly suppressed, although not zeroed, in grazing incidence geometry and horizontal polarization.

The polarization and angular dependence of O K-edge XAS is determined by the O $2p$-Ir $5d$ t_{2g} hybridization strength, and the dipole matrix element governing the O $1s$-$2p_i$ transitions ($i = x$, y, and z). Figure 3(a) shows the

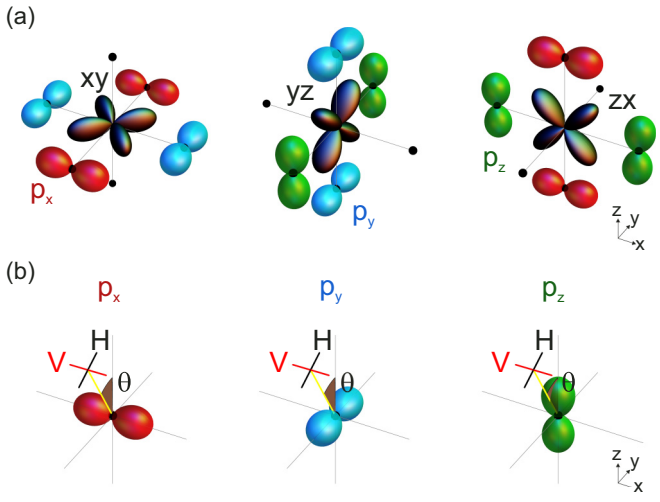

FIG. 3. (Color online) (a) Sketch of the O $2p_i$-Ir $5d$ t_{2g} orbital dependent hybridizations, and (b) of the different O $2p_i$ orbitals ($i = x$, y, and z) orientations with respect to the incoming photon polarization. The incidence angle θ is also indicated.

O $2p_i$-Ir $5d$ t_{2g} orbital dependent hybridizations; the xy orbital has a finite overlap with four in-plane O $2p_x$ and $2p_y$ orbitals, while the yz (zx) orbital hybridizes with two apical O $2p_y$ ($2p_x$) and two in-plane O $2p_z$ ($2p_z$) orbitals. The strength of the hybridization, however, depends on the Ir-O bond length r, which is different for the in-plane and apical oxygens: Here we assume a power-law dependence of the hybridization strength on r, i.e., $r^{-\alpha}$, where $\alpha = 3.5$ [26]. From Fig. 3(b) one can understand the angular and polarization dependence of the O $1s$-$2p_i$ matrix elements, which, because of the isotropy of the O $1s$ orbital, is fully determined by the relative orientation of the polarization vector and the O $2p_i$ orbitals. It follows that the transitions to the O $2p_x$, $2p_y$, and $2p_z$ orbitals have θ dependencies of 0, $\cos^2\theta$, and $\sin^2\theta$ for horizontal polarization, and 1, 0, and 0 for vertical polarization, respectively. Therefore, the intensity of the feature associated with the in-plane oxygens has a θ dependence of $n_{xy}\cos^2\theta + 2n_{yz}\sin^2\theta$ for horizontal polarization, and n_{xy} for vertical polarization. Here n_{xy} and $n_{yz} = n_{zx}$ are the orbital occupancies of the xy and yz or zx states, respectively ($n_{xy} + n_{yz} + n_{zx} = 1$ in the case of Ir^{4+}). On the other hand, the intensity of the feature associated with the apical component is given by $1.07^{-\alpha}n_{yz}\cos^2\theta$ for horizontal polarization, and $1.07^{-\alpha}n_{yz}$ for vertical polarization, where the factor $1.07^{-\alpha} \approx 80\%$ comes from the 7% elongation of the IrO_6 octahedra. To summarize these arguments, no angular dependence is expected in the case of vertical polarization, in agreement with the experimental findings, while the intensity of the in-plane and apical oxygens contributions are proportional to n_{xy} and n_{yz}, respectively. In the case of horizontal polarization, instead, an angular dependence is expected: Specifically, at normal incidence ($\theta = 0$) the intensity is identical to the vertical polarization case, while at $\theta = 80^\circ$ the in-plane and apical oxygens contribution are proportional to $0.03n_{xy} + 0.97(2n_{yz})$ and $1.07^{-\alpha}0.03n_{yz}$, respectively. These considerations allow us to extract the occupancies of the xy, yz, and zx orbitals, in terms of (fraction of) *holes*, from the polarization and angular dependence of O K-edge XAS (Fig. 2). We obtain $n_{xy} = 0.37 \pm 0.04$ and $n_{yz} = n_{zx} = 0.31 \pm 0.02$. Although there appears to be a slightly higher occupancy of the xy orbital ($\Delta \gtrsim 0$), this result is also consistent with an almost even occupation of the xy, yz, and zx orbitals ($n_{xy} = n_{yz} = n_{zx} = 1/3$), suggesting that Ba_2IrO_4 belongs to the class of $j_{\text{eff}} = \frac{1}{2}$ iridates.

Knowledge of the orbital occupancies allow us in turn to estimate the *effective* tetragonal crystal field splitting Δ [see Eq. (1) and related text]. However, for this we first require a precise determination of the spin-orbit coupling ζ. We can then use the fact that the occupancies of the xy, yz, and zx orbitals are given by $n_{xy} = C_0^2/(C_0^2 + 2)$ and $n_{yz} = n_{zx} = 1/(C_0^2 + 2)$, respectively, where the dependence on Δ and ζ is parametrized in C_0. An estimate of the spin-orbit coupling constant can be extracted from O K-edge RIXS data. Figure 4 shows a representative O K-edge RIXS spectrum of Ba_2IrO_4 for photons impinging on the sample with an angle $\theta = 25^\circ$ (specular geometry). The spectrum shows a clear elastic line at zero energy loss and the first distinct feature is found at 0.64 eV. Higher energy features have the characteristics of resonant fluorescence emission, as verified by inspecting their incident photon energy dependence. The incident photon

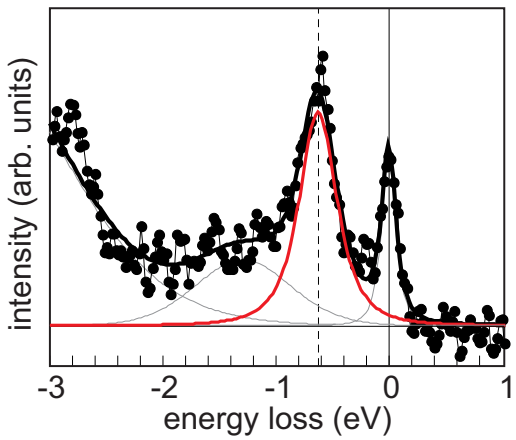

FIG. 4. (Color online) O K-edge RIXS spectrum of Ba_2IrO_4 for photons impinging at the sample with an angle $\theta = 25^\circ$ (red open circles). Solid lines are the corresponding fitting curves used to determine the peak position.

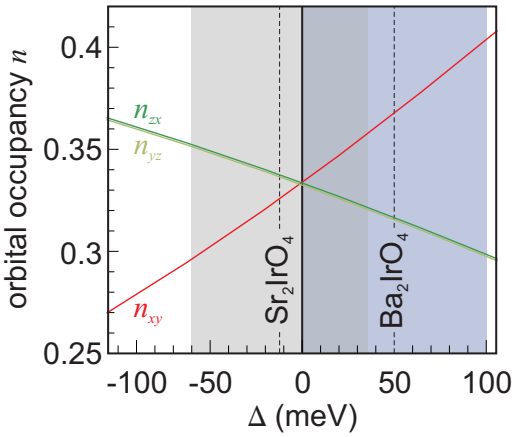

FIG. 5. (Color online) Calculated orbital occupancies of the xy, yz, and zx orbitals as a function of the tetragonal crystal field splitting Δ, for $\zeta = 0.43$ eV. The shaded areas indicate the estimated range of Δ in Ba_2IrO_4, as extracted by the current experiment, and in Sr_2IrO_4 [19].

energy was fixed at 530.1 eV, i.e., the energy corresponding to the in-plane oxygen contribution in the O K-edge XAS spectra; doing so, we expected to maximize the intensity of RIXS transitions involving orbitals hybridized with the Ir 5d t_{2g} states. Therefore, in analogy to Ir L_3-edge RIXS, we assign this transition to the excitation of the hole from the $j_{\rm eff} = \frac{1}{2}$ ground state to the $j_{\rm eff} = \frac{3}{2}$ band. In a single ion picture [5–9] the energy cost for this transition is $3\zeta/2$, from which the value of the spin-orbit coupling constant ζ is estimated to be 0.43 eV. This value remarkably agrees with the estimate of the spin-orbit coupling in Ba_2IrO_4 ($\zeta = 0.42$ eV) given in [14], based on the Ir L_2 and L_3 XAS branching ratio.

Figure 5 shows the calculated dependence of the orbital occupancies on the tetragonal crystal field for $\zeta = 0.43$ eV. For the derived values of the orbital occupancies given above, we calculate an *effective* tetragonal crystal field of 50 meV, with relatively tight constraints related to the error bars in the estimate of the XAS peak intensities, i.e., $0 \leqslant \Delta \leqslant 100$ meV. This result may be compared with the recent work of Boseggia *et al.* [19] on Sr_2IrO_4 who found that $-60 \leqslant \Delta \leqslant 35$ meV based on the accurate determination of the magnetic moment direction relative to the octahedra rotation by XRMS. Figure 5 compares the estimated tetragonal crystal field splittings in Sr_2IrO_4 and Ba_2IrO_4. One can speculate that $\Delta \gtrsim 0$ in Ba_2IrO_4, while $\Delta \lesssim 0$ in Sr_2IrO_4, i.e., the *effective* tetragonal crystal field has opposite sign in the two compounds. Although one can intuitively explain this difference by invoking the elongation of the IrO_6 octahedra, which is more pronounced in Ba_2IrO_4 than in Sr_2IrO_4, and thus favors the occupancy of the xy orbital, it should be noted that this result contradicts recent theoretical calculations by Katukuri *et al.* [21]. Indeed, a recent LDA + DMFT study predicts the effective tetragonal crystal field in Sr_2IrO_4 to be negative and that an additional elongation of the c axis is required to recover the SU(2) limit [27].

In summary, we demonstrate how the combination of soft x-ray techniques yields more information than any one technique used in isolation, allowing us in this case to understand the link between structural distortions (octahedral rotation and elongation) and the $j_{\rm eff} = \frac{1}{2}$ ground state in iridates. By exploiting x-ray linear dichroism at the O K absorption edge of the prototypical perovskite iridate Ba_2IrO_4, we have determined the orbital occupancies of Ir^{4+} 5d ground state to be $n_{xy} = 0.37 \pm 0.04$ and $n_{yz} = n_{zx} = 0.31 \pm 0.02$. An estimate of the *effective* tetragonal distortion to the cubic crystal field splitting is given by extracting the spin-orbit coupling constant ($\zeta = 0.43$ eV) from O K-edge RIXS measurements. The result is that $\Delta = 50(50)$ meV, i.e., very small compared with the cubic crystal field in Ba_2IrO_4 of about 3 eV. We conclude that Ba_2IrO_4 may be classified as a spin-orbit Mott insulator, with a ground state close to the ideal $j_{\rm eff} = \frac{1}{2}$ state proposed to give rise to the novel properties of iridates. We hope that the quantitative information provided by our analysis will help refine future theoretical approaches and act as a guide to the large community of "material engineers" which exploits structural distortions to tune material properties.

H. M. Rønnow acknowledges support from the Swiss National Science Foundation and its Sinergia network "Mott Physics Beyond the Heisenberg Model." Work in London was supported by EPSRC.

[1] S. J. Moon, H. Jin, K. W. Kim, W. S. Choi, Y. S. Lee, J. Yu, G. Cao, A. Sumi, H. Funakubo, C. Bernhard, and T. W. Noh, Phys. Rev. Lett. **101**, 226402 (2008).

[2] B. J. Kim, H. Jin, S. J. Moon, J. Y. Kim, B. G. Park, C. S. Leem, J. Yu, T. W. Noh, C. Kim, S. J. Oh, J. H. Park, V. Durairaj, G. Cao, and E. Rotenberg, Phys. Rev. Lett. **101**, 076402 (2008).

[3] M. K. Crawford, M. A. Subramanian, R. L. Harlow, J. A. Fernandez-Baca, Z. R. Wang, and D. C. Johnston, Phys. Rev. B **49**, 9198 (1994).

[4] H. Okabe, M. Isobe, E. Takayama-Muromachi, A. Koda, S. Takeshita, M. Hiraishi, M. Miyazaki, R. Kadono, Y. Miyake, and J. Akimitsu, Phys. Rev. B **83**, 155118 (2011).

[5] L. J. P. Ament, G. Khaliullin, and J. van den Brink, Phys. Rev. B **84**, 020403 (2011).

[6] X. Liu, V. M. Katukuri, L. Hozoi, W.-G. Yin, M. P. M. Dean, M. H. Upton, J. Kim, D. Casa, A. Said, T. Gog, T. F. Qi, G. Cao, A. M. Tsvelik, J. van den Brink, and J. P. Hill, Phys. Rev. Lett. **109**, 157401 (2012).

[7] K. Ohgushi, J.-i. Yamaura, H. Ohsumi, K. Sugimoto, S. Takeshita, A. Tokuda, H. Takagi, M. Takata, and T.-h. Arima, Phys. Rev. Lett. **110**, 217212 (2013).

[8] L. Hozoi, H. Gretarsson, J. P. Clancy, B.-G. Jeon, B. Lee, K. H. Kim, V. Yushankhai, P. Fulde, Y.-J. Kim, and J. van den Brink, arXiv:1212.4009.

[9] M. Moretti Sala, S. Boseggia, D. F. McMorrow, and G. Monaco, Phys. Rev. Lett. **112**, 026403 (2014).

[10] B. J. Kim, H. Ohsumi, T. Komesu, S. Sakai, T. Morita, H. Takagi, and T. Arima, Science **323**, 1329 (2009).

[11] J. W. Kim, Y. Choi, J. Kim, J. F. Mitchell, G. Jackeli, M. Daghofer, J. van den Brink, G. Khaliullin, and B. J. Kim, Phys. Rev. Lett. **109**, 037204 (2012).

[12] S. Boseggia, R. Springell, H. C. Walker, A. T. Boothroyd, D. Prabhakaran, D. Wermeille, L. Bouchenoire, S. P. Collins, and D. F. McMorrow, Phys. Rev. B **85**, 184432 (2012).

[13] S. Boseggia, R. Springell, H. C. Walker, A. T. Boothroyd, D. Prabhakaran, S. P. Collins, and D. F. McMorrow, J. Phys.: Condens. Matter **24**, 312202 (2012).

[14] S. Boseggia, R. Springell, H. C. Walker, H. M. Rønnow, C. Rüegg, H. Okabe, M. Isobe, R. S. Perry, S. P. Collins, and D. F. McMorrow, Phys. Rev. Lett. **110**, 117207 (2013).

[15] S. Calder, G.-X. Cao, S. Okamoto, J. W. Kim, V. R. Cooper, Z. Gai, B. C. Sales, M. D. Lumsden, D. Mandrus, and A. D. Christianson, Phys. Rev. B **89**, 081104(R) (2014).

[16] L. C. Chapon and S. W. Lovesey, J. Phys.: Condens. Matter **23**, 252201 (2011).

[17] K. Ishii, I. Jarrige, M. Yoshida, K. Ikeuchi, J. Mizuki, K. Ohashi, T. Takayama, J. Matsuno, and H. Takagi, Phys. Rev. B **83**, 115121 (2011).

[18] J. Kim, D. Casa, M. H. Upton, T. Gog, Y.-J. Kim, J. F. Mitchell, M. van Veenendaal, M. Daghofer, J. van den Brink, G. Khaliullin, and B. J. Kim, Phys. Rev. Lett. **108**, 177003 (2012).

[19] S. Boseggia, H. C. Walker, J. Vale, R. Springell, Z. Feng, R. S. Perry, M. Moretti Sala, H. M. Rønnow, S. P. Collins, and D. F. McMorrow, J. Phys.: Condens. Matter **25**, 422202 (2013).

[20] S. Moser, L. Moreschini, A. Ebrahimi, B. Dalla Piazza, M. Isobe, H. Okabe, J. Akimitsu, V. V. Mazurenko, K. S. Kim, A. Bostwick, E. Rotenberg, J. Chang, H. M. Rønnow, and M. Grioni, arXiv:1310.1307.

[21] V. M. Katukuri, H. Stoll, J. van den Brink, and L. Hozoi, Phys. Rev. B **85**, 220402 (2012).

[22] S. J. Moon, M. W. Kim, K. W. Kim, Y. S. Lee, J.-Y. Kim, J.-H. Park, B. J. Kim, S.-J. Oh, S. Nakatsuji, Y. Maeno, I. Nagai, S. I. Ikeda, G. Cao, and T. W. Noh, Phys. Rev. B **74**, 113104 (2006).

[23] C. T. Chen, F. Sette, Y. Ma, M. S. Hybertsen, E. B. Stechel, W. M. C. Foulkes, M. Schluter, S.-W. Cheong, A. S. Cooper, L. W. Rupp, B. Batlogg, Y. L. Soo, Z. H. Ming, A. Krol, and Y. H. Kao, Phys. Rev. Lett. **66**, 104 (1991).

[24] M. Schmidt, T. R. Cummins, M. Bürk, D. H. Lu, N. Nücker, S. Schuppler, and F. Lichtenberg, Phys. Rev. B **53**, R14761 (1996).

[25] T. Mizokawa, L. H. Tjeng, G. A. Sawatzky, G. Ghiringhelli, O. Tjernberg, N. B. Brookes, H. Fukazawa, S. Nakatsuji, and Y. Maeno, Phys. Rev. Lett. **87**, 077202 (2001).

[26] W. Harrison, *Electronic Structure and the Properties of Solids: The Physics of the Chemical Bond* (Dover, New York, 1989).

[27] H. Zhang, K. Haule, and D. Vanderbilt, Phys. Rev. Lett. **111**, 246402 (2013).